

## JUMBO TORNADO OUTBREAK OF 3 APRIL 1974

T. Theodore Fujita  
Department of the Geophysical Sciences  
The University of Chicago

Extraordinary tornado outbreak of April 3 may be called the "Jumbo outbreak", because the combination of the year 74 and the 3rd day of April or the 4th month of the year, results in the numbers 747 which designate Jumbo Jet. Following the Jumbo outbreak, an extensive aerial survey was performed in cooperation with the National Severe Storms Laboratory and the University of Oklahoma.

### TOTAL PATH MILEAGE OF TORNADOES

Date	Outbreak	Total Path Mileage	No. of Tornadoes	Deaths
18 March 1925	Tri-state tornado outbreak	437	7	746
11 April 1965	Palm Sunday outbreak	853	31	256
3 April 1974	Jumbo outbreak	2014	93	330
Year 1971 in entire U. S.		4126	888	154
Year 1972 in entire U. S.		2431	740	22
Year 1973 in entire U. S.		5306	1108	86

The areal survey revealed that the total path length of tornadoes in the eleven state area was in excess of 2000 miles. Statistics during the past three years indicate that the total path mileage of U. S. tornadoes is approximately 4000 miles per year. Just about one-half of this total path mileage occurred within an 18-hour period beginning at 2 PM CDT on April 3. Tornado paths were found in unexpected locations such as in deep canyons, and on steep slopes of mountains (see Fig. 1). Aerial-survey participants experienced

considerable difficulties in photographing damage while flying low over rugged terrain especially in the afternoon hours. About 3600 color pictures were taken for use in mapping the damage paths.

The tornado path map presented in Fig. 2 reveals that the Jumbo outbreak was 3 times more extensive than the Palm Sunday outbreak (Fig. 3). However, it was very fortunate that most of the intense tornadoes avoided the large cities with the exception of Xenia, Ohio (storm No. 24). The Guin tornado (No. 75) left a 132-mile path which cut through the center of Guin, Alabama. Fortunately, the storm weakened as it moved toward the city of Huntsville. The tornado, then, climbed to the top of Monte Sano Mountain (1640 ft) and descended on the northeast slope while intensifying significantly.

Mountain-climbing and canyon-crossing paths were found at numerous locations in Kentucky, Tennessee, Georgia, North Carolina, Virginia, and West Virginia. Blue Ridge tornado (No. 82) formed in the mountain just east of Mulberry Gap, 1800 ft MSL and crossed a 3000 ft ridge before moving down to the bottom of a deep canyon. The tornado finally climbed to the 3300 ft top of Rich Knob. Numerous trees were uprooted or clipped as the storm descended toward the village of Colwell where a number of houses in the valley were smashed. Little variation in the direction of the tornado path was found in the rugged terrain, giving an impression that the tornado moved along the path as determined by the parent cloud and not by the topography.

The path-length and path-width scale of 93 tornadoes were determined based exclusively on aerial mapping and photography, while the F-scale intensity was supplied by the local Weather Service Forecast Offices. Where no F-scale is available from WSFO at this time, aerial pictures were used for the preliminary scale determination.

FPP distributions of 93 tornadoes are shown in Fig. 4. There are reports of one F6 and five F5 tornadoes. The Xenia tornado (No. 24) is rated as F6 while F5 tornadoes are identified as Hamburg tornado (No. 23), Depauw tornado (No. 27), Sayler Park tornado (No. 30), Brandenburg tornado (No. 33), and Guin tornado (No. 75). It should be noted, however, that these F scale ratings are the result of visual inspection of damage with expected accuracy of  $\pm$  one scale. Both lengths and mean widths, as expressed by the PP scale, turned out to be just about one order of magnitude larger than the average U. S. tornadoes, revealing that the Jumbo-outbreak tornadoes were unusually intense, long, and wide. For FPP scale, refer to Fujita (1973).

Diurnal variation of tornadoes was obtained by counting the number of tornadoes which were in progress during each hour. As shown in Fig. 5, 16 tornadoes, of which 4 were rated as F4 or F5, occurred in a one hour period, 4-5 PM. Six F4 tornadoes along with a total of 23 storms occurred between 7-8 PM followed by a gradual decrease in both number and intensity.

Although the activity was insignificant during the midnight hours, 3 tornadoes (Nos. 89, 90, and 92) occurred in West Virginia and Virginia between 3 and 4 AM of the 4th.

ATS pictures taken during the afternoon hours show three major squall lines oriented in the SW-NE direction. In fact, most of the tornado outbreak took place inside these squall lines.

Three squall lines in their development stage are clearly identifiable in the 1352 CDT picture. The northern line was located between Saint Louis and Chicago, covering central Illinois. The central line extended from northwestern Kentucky to central Indiana while the southern line was seen along the Tennessee, North Carolina border.

Each of the squall lines grew explosively shortly before 1400 CDT, giving rise to the formation of tornadoes at Lincoln, Illinois, at 1408 CDT (No. 1) and Cleveland, Tennessee at 1410 CDT (No. 77). Ten minutes later, at 1420 CDT, the Jonesville tornado (No. 22) and the Depauw tornado (No. 27) touched down from the central squall line, thus signaling the beginning of the Jumbo outbreak over the 11 state areas.

An ATS picture at 1617 CDT includes the paths of 16 tornadoes which occurred between 1600-1700 CDT (Fig. 6). Most tornadoes moved northeastward at 40 to 60 mph while squall lines were advancing toward the southeast. As expected, tornadoes moved with individual cells not with squall lines.

Numerous hook echoes were reported from various radar stations. During the peak periods of the outbreak, the number of reported hook echoes exceeded that of tornadoes. It is partly because an apparent hook does not always represent the true hook echo. Moreover, there were a large number of hook echoes which failed to produce tornadoes during their lifetime.

Shown in Fig. 7 are three echoes depicted by WSR-57 radar at Evansville, Indiana. The picture was made by combining a full-gain picture with a reduced-gain

picture in black. At the time of this picture, both the Janesville tornado (No. 22) and the Depauw tornado (No. 27) touched down from echoes A and C, respectively. Echo B never produced a tornado during its lifetime. The overall shape of echo B represents a typical hook echo. When the south end of the hook is examined in detail, however, its tip bends anticyclonically toward the northwest. A similar anticyclonic tip is seen near the western edge of echo C. The picture presented herein indicates that the higher the resolution the more complicated is the circulation patterns.

A recent report of the April 3, 1974 tornadoes by Changnon and Morgan (1974) presents a typical hook echo which did not produce F1 or stronger tornado, although high winds were accompanied by the cell (Fig. 8).

Cycloidal marks such as have been reported by Van Tassel (1955), Prosser (1964), and Fujita, Bradbury and Black (1970) were found in open fields within the paths of a number of tornadoes in several states.

A typical cycloidal mark, photographed in the path of Anchor tornado (No. 2), is shown in Fig. 9. Cycloidal marks such as these consist of a low pile of corn stubble and small debris gathered by suction vortices. A model of suction vortices which produce bands of debris deposit appears in a survey paper by Fujita (1971). Since a cycloidal mark in an open field consists of small-pieced debris, the mark is lighter than the ground when viewed from the sunny side. From the shady side, black cycloidal marks are seen instead. It is of interest to observe the brightness changes as an airplane circles around over a cycloidal mark.

The characteristics of a cycloidal mark can be used in computing the tangential speed of a suction vortex moving around the tornado center. The tangential speed of suction vortices which gave rise to the cycloidal mark in Fig. 9 was computed from Fig. 84 in the Palm Sunday tornado paper by Fujita, Bradbury and Van Thullenar (1970). The result indicates that the tangential speed of 90 mph decreased to about 70 mph while approaching the highway. Upon crossing the highway, the tangential speed increased to about 120 mph. The maximum translational speed of the suction vortex occurring on the right side of the path is obtained by adding 60 mph, the translational speed of the tornado. Such a simple calculation leads to a conclusion that the translational speed of suction vortices decreased from 150 mph to 130 mph and then increased to 180 mph along the path in Fig. 9.

The maximum windspeed to be used as the bases of the F-scale estimate should be faster than above speeds because each suction vortex rotates around its vertical axis. With a conservative rotational speed of suction vortices being 20 mph, then the maximum windspeed of Anchor tornado will be  $180 + 20 \text{ mph} = 200 \text{ mph}$ . This speed corresponds to the uppermost F3 scale.

Although a shallow debris deposit takes place along a cycloidal track in an open field, a complete destruction of trees occurs in a forest. Within Tallahoma tornado path (No. 69) in southern Tennessee, cycloidal marks in the plowed field extended into a pine forest where trees were literally flattened along cycloidal tracks.

Suction vortices in action were filmed by Mr. Wally Hubbard, a WISH-TV News cameraman-correspondent. The film reveals the features of 2 to 4 suction vortices rotating around the center of Muncie tornado (No. 21). Initially, the tornado was accompanied by a large funnel reaching the ground. In a couple of minutes, the bottom of the funnel lifted, thus exposing small vertical funnels extending down along the axis of the suction vortices (Fig. 10).

Each of the suction vortices was rotating rather rapidly. It is fortunate to find that a number of aerial pictures were taken after the storm over the area of Hubbard's movie. An attempt is now being made to combine the movie with aerial photographs. This study will be useful in learning the two scales of circular motions within a tornado. It should be noted that similar vortices were produced by Ward (1970) in his laboratory model.

Three-scale vortices involving tornado cyclone, tornado, and suction vortex now appear to be important toward the solution of tornado problems. Schematic paths of the center of these vortices are shown in Fig. 11, along with the definition of the path direction measured counterclockwise from east.

The path of a tornado-cyclone center is relatively smooth with its direction,  $\alpha$  varying slowly with time. On the other hand,  $\beta$ , the direction of tornado center changes from  $\beta_1$ , the touch-down direction to  $\beta_2$ , the lift-off direction. Now, the turn angle of a tornado is defined as

$$\beta_2 - \beta_1 = \Delta\beta \quad , \text{ the turn angle}$$

$$\Delta\beta > 0 \quad , \text{ left-turn tornado}$$

$$\Delta\beta \cong 0 \quad , \text{ no-turn tornado}$$

$$\Delta\beta < 0 \quad , \text{ right-turn tornado}$$

Most tornadoes in the Jumbo outbreak were left-turn tornadoes with their paths curving toward the north prior to their dissipation (see Fig. 2).

Naturally, the variation of  $\mathcal{T}$ , the direction of a suction vortex, is extremely large, changing  $360^\circ$  within a very short distance.

All participants in our aerial survey of the Jumbo outbreak were briefed on the basic characteristics of these three-scales of motions. Some tornado paths inside an overlapping area of survey responsibility were mapped three times, unknowingly and independently, by different participants. The results of each of the three surveys were found to be very close to each other, proving the high degree of mapping accuracy performed by the participants.

Frequencies of left-turn tornadoes in the Jumbo outbreak were significantly higher than those of right-turn tornadoes. Of the 65 tornadoes with a 10 mile or longer path length, 43 were left-turn tornadoes. According to the statistics presented in Fig. 12, left-turn tornadoes are more intense than their right-turn counterparts. The mean F-scale intensity of right-turn tornadoes is about F 3.0, while the mean intensity of left-turn tornadoes increases from F 3 to about F 4 as the turn angle increases to about  $60^\circ$ . This evidence implies that a strong tornado moves far into the front sector of the tornado cyclone, while a weak tornado dissipates before making an appreciable left turn.

Left-turn tornadoes often touch down in the direction of the parent tornado cyclone. Figure 12 reveals such a tendency. As the turn angle increases, however, the touch-down direction deviates further to the right.

On the other hand, right-turn tornadoes tend to touch down in the right forward quadrant of the parent tornado cyclone. These turning characteristics were found in many cases during the aerial survey.

Models of damage paths were constructed based on aerial inspections and photographs taken over the 93 tornado paths. Converging patterns of damaged trees are commonly observed on the immediate up-wind side of the touch-down point. Also observed are the divergence patterns on the down-wind side of the lift-off point.

Participants in the aerial survey equally received a definite impression that the path of a left-turn tornado disappears as soon as the path direction increases to about 60 or 30 azimuth (Fig. 13). Cycloidal marks and convergence lines of trees and debris were carefully checked in an effort to map the locus of the tornado center.

As shown in Fig. 14, the touch-down point of a right-turn tornado is located several miles to the right of the tornado-cyclone path. Usually, the tornado path approaches the tornado-cyclone path as the tornado advances. The direction of high winds near the lift-off point is, more or less, parallel to that of the tornado cyclone.

Expected locations of tornadoes within a tornado cyclone are presented in Fig. 15, which was constructed by combining radar pictures and damage paths. The three well-known features of hook echoes, rotating thunderstorms, and tornado cyclones were taken into consideration in drawing the figure.

The rotation axis of a rotating thunderstorm coincides with that of the tornado cyclone, characterized by the field of low pressure, the rotating updraft as well as the twisting downdraft. Since the forward side of a tornado cyclone is dominated by an intense updraft, the downdraft air and precipitation particles have a tendency to wrap around the center from the back side, thus producing a hook echo on PPI scope. Letters "L" and "R" in the figure denote the locations where left-turn and right-turn tornadoes are likely to form.

An intense tornado often remains over a fixed location relative to the tornado cyclone center, where the microscale field of surface vorticity and convergence is predominant. Such a tornado moves side by side with the tornado-cyclone center without changing its relative position.

Family tornadoes are defined as those spawned from a single tornado cyclone. A family of 5 was documented by Fujita (1960) in his study of the Fargo tornadoes. Darkow (1971) reported 5 families, each with 5 tornadoes. Six tornadoes in a family moved from near Lafayette, Indiana to Cleveland, Ohio during the Palm Sunday outbreak (see Fig. 3).

There were two significant family tornadoes in the Jumbo outbreak. They are the Monticello Family in Indiana and Ohio, and the Cincinnati Family extending over a tri-state area (Fig. 16).

The first four members of the Monticello family (Nos. 4 through 7) are relatively weak and short with their FPP being 2 2 2, 2 3 2, 2 2 2, and 3 3 3. They were right-turn tornadoes. The fifth one which hit the downtown area of Monticello is rated as 4 5 3 with a path length of 118 miles. The sixth was a short lived tornado.

All of the six tornadoes (Nos. 27 through 32) spawned as the Cincinnati family (Fig. 16) were left-turn tornadoes. Of extreme interest is the successive decrease in the path length. The first one or the Depauw tornado (No. 27) was rated as 5 4 4 while the last one (No. 32) was as weak as 2 2 2.

Why is it that the Monticello family consisted predominantly of right-turn tornadoes while the entire Cincinnati family consisted of left-turn tornadoes? This question remains to be answered. Nonetheless, the major difference in the characteristics of tornadoes belonging to each tornado family gives an impression that the characterization of a tornado cyclone is important in understanding the dynamics of tornado formations. It has been planned that all tornadoes in the Jumbo outbreak be examined in detail along with the characteristics of parent echoes.

Tornado-cyclone brothers were found while investigating a series of four tornadoes: Nos. 80, 81, 82, and 83. Initially, all storms in Fig. 17 were assumed to be a family of 4 tornadoes. Careful examination of radar pictures revealed unexpectedly that the first and the second tornadoes were produced by tornado cyclone I while the third and fourth spawned out of tornado cyclone II.

The distance between tornado cyclones I and II was so short that they were rotating around their common center. For typhoons, such an interaction has been known as Fujiwara effect. In astronomy, a system of double stars rotates around their common center of gravity.

Tornado cyclones, which are rotating around each other under the influence of their induced vortices, may be called tornado-cyclone brothers. From this point of view, the Resaca and Blue Ridge tornadoes are cousin tornadoes whose parents are brothers.



Conclusions: The Jumbo outbreak of tornadoes on April 3-4, 1974 in terms of the total number and the path mileage was more extensive than all known outbreaks. Besides, the tornado characteristics were found to include many important aspects such as multiple suction vortices, family tornadoes, and cousin tornadoes spawned from interacting tornado cyclones. Thus, the basic data collected through a detailed aerial survey will provide us with a rich gold mine toward the solution of various scales of rotating motions, leading to the prediction and warning of tornadoes.

Acknowledgements: The research presented herein has been sponsored by the National Oceanic and Atmospheric Administration, NESS, under grant 04-4-158-1 and by the National Aeronautics and Space Administration under grant NGR 14-001-008. The aerial survey was performed by the following personnel: Fujita, Pearl, Tecson, Forbes, Pasken, La Placa and Sereno (The University of Chicago); Golden and Lemon (National Severe Storms Laboratory); and McCarthy (University of Oklahoma).

## REFERENCES

- Changnon, S. A. and G. M. Morgan (1974): Unique hail and tornadic storm observations in Central Illinois and Eastern Indiana on 3 April 1974. Prelim. Report. Ill. State Water Survey, 6 pp.
- Darkow, G. L. (1971): Periodic Tornado Production by Long-lived Parent Thunderstorms. Preprints of papers presented at the Seventh Conference on Severe Local Storms, October 5-7, 1971, Kansas City, Mo., pp 214-217.
- Fujita, T. T. (1960): A detailed analysis of the Fargo tornadoes of June 20, 1957. Res. Paper No. 42, U. S. Weather Bureau, 67 pp.
- \_\_\_\_\_, D. L. Bradbury and P. G. Black (1967): Estimation of Tornado Wind Speeds from Characteristic Ground Marks. SMRP Res. Paper No. 69, The University of Chicago, 19 pp.
- \_\_\_\_\_, D. L. Bradbury and C. F. Van Thullenar (1970): Palm Sunday Tornadoes of April 11, 1965. Mon. Wea. Rev., 98, No. 1, pp 29-69.
- \_\_\_\_\_, (1971): Proposed Mechanism of Suction Spots accompanied by Tornadoes. Preprints of papers presented at the Seventh Conference on Severe Local Storms, October 5-7, 1971, Kansas City, Mo., pp 208-213.
- \_\_\_\_\_, (1973): Tornadoes Around the World. Weatherwise, 26, pp 56-62, 78-83.
- Prosser, N. E. (1964): Aerial Photographs of a Tornado Path in Nebraska, May 5, 1964. Mon. Wea. Rev., 92, No. 12, 593-598.
- Van Tassel, E. L. (1955): The North Platte Valley Tornado Outbreak of June 27, 1955. Mon. Wea. Rev., 83, No. 11, 255-264.
- Ward, Neil B. (1970): The Exploration of Certain Features of Tornado Dynamics Using a Laboratory Model. NOAA Tech. Memo. ERLTM-NSSL 52, National Severe Storms Lab., Norman, Okla., 22 pp.

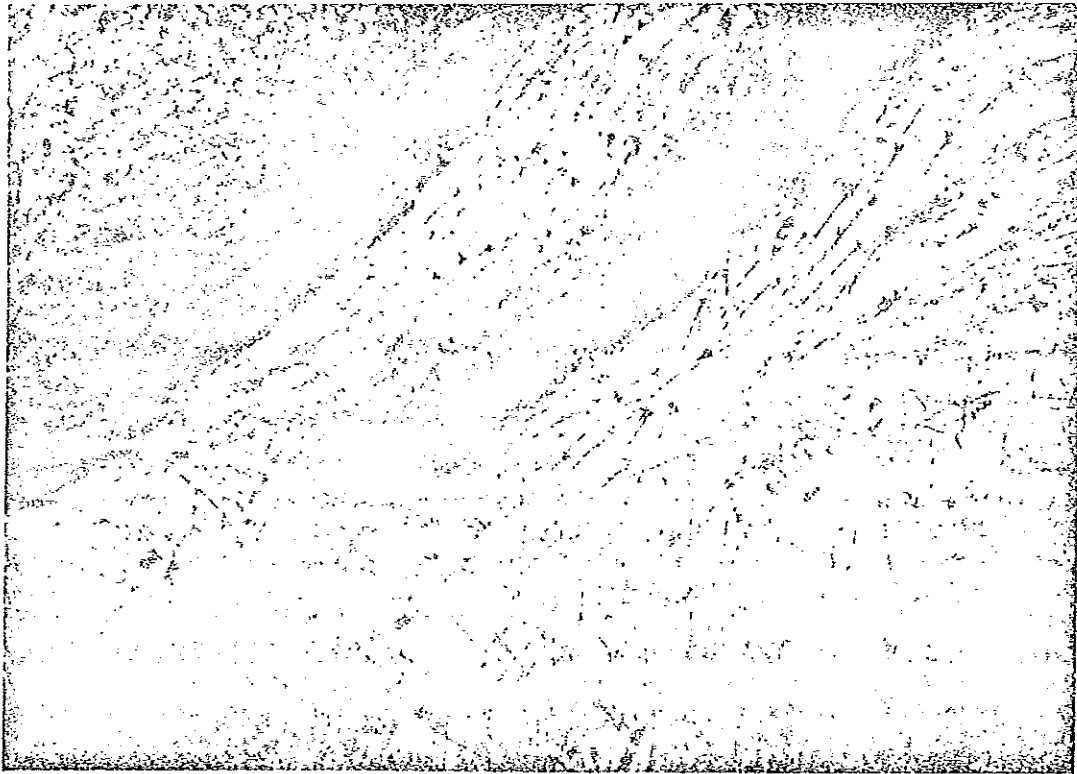


Fig. 1. Uprooted trees in steep mountain south of Murphy, N. C. Tornado moved from right to left.

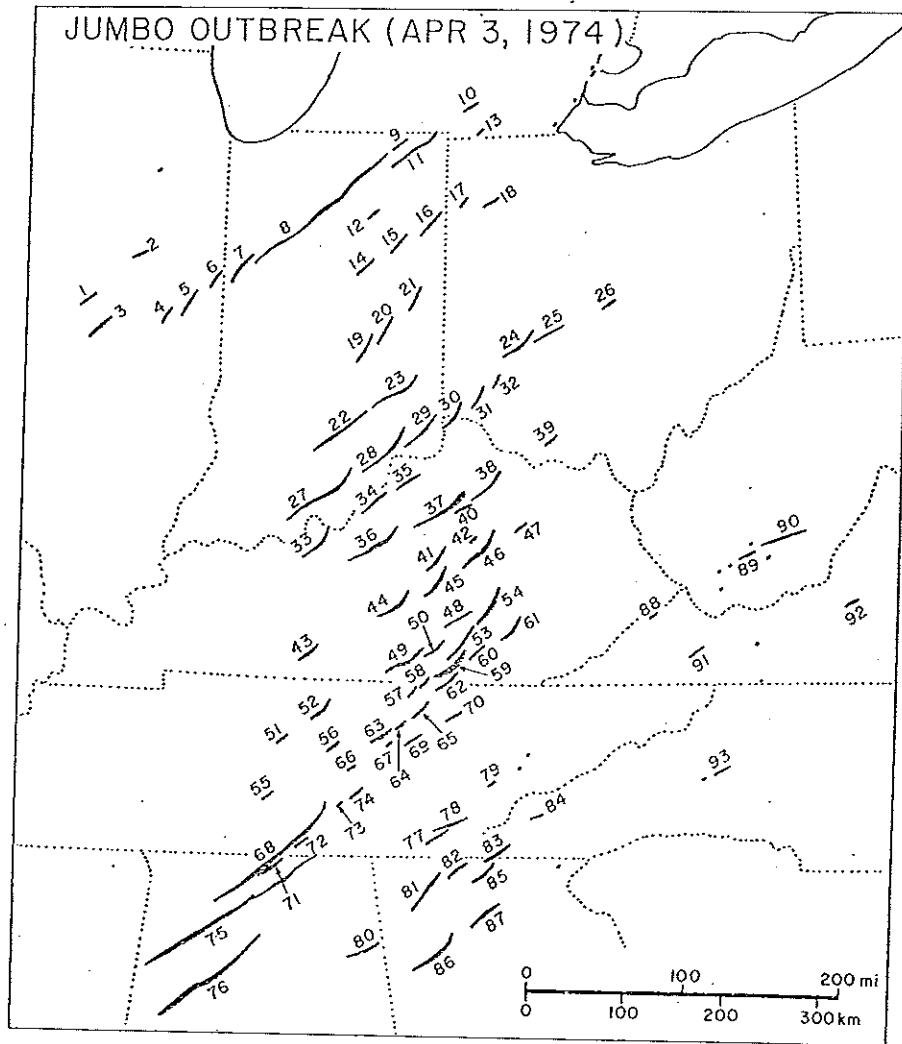


Fig. 2. Paths of 93 tornadoes on the day of Jumbo outbreak. Tornadoes with FPP scale larger than 111 are numbered, 1 through 93.

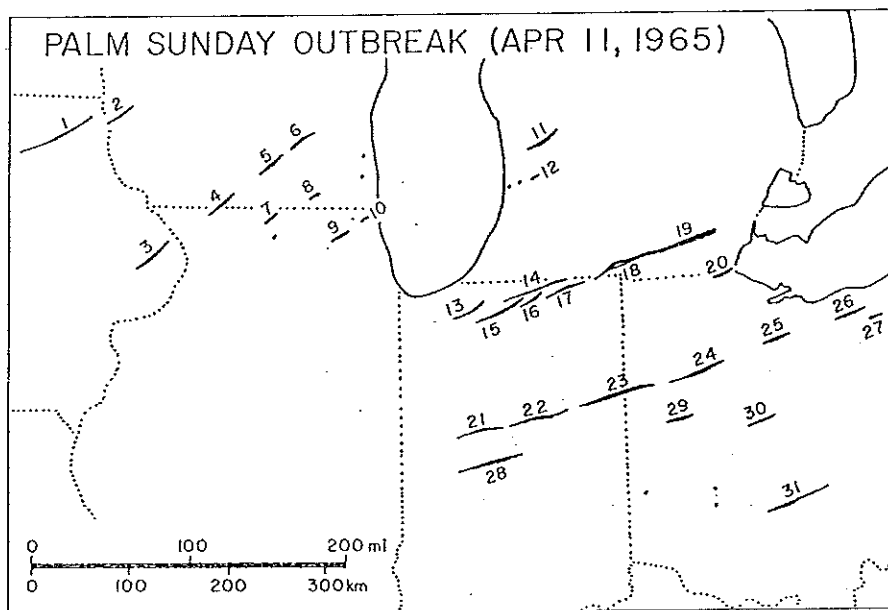


Fig. 3. Path and identification numbers of 31 tornadoes with FPP larger than 111. April 11-12, 1965. From Fujita et al. (1970).

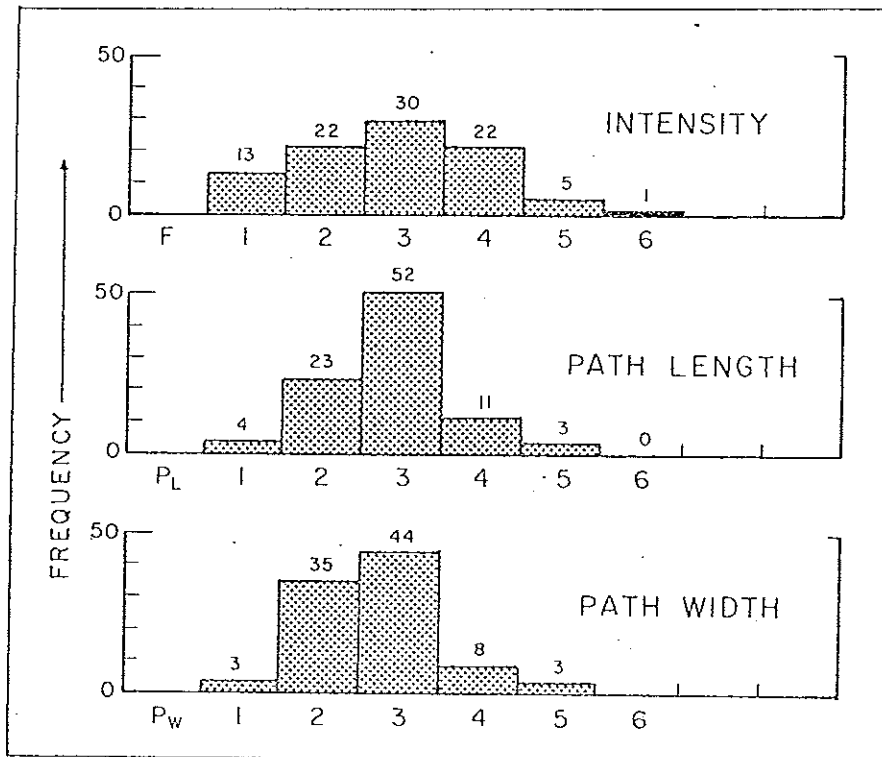


Fig. 4. Distribution of tornado intensity, path length, and mean path width.  
April 3-4, 1974.

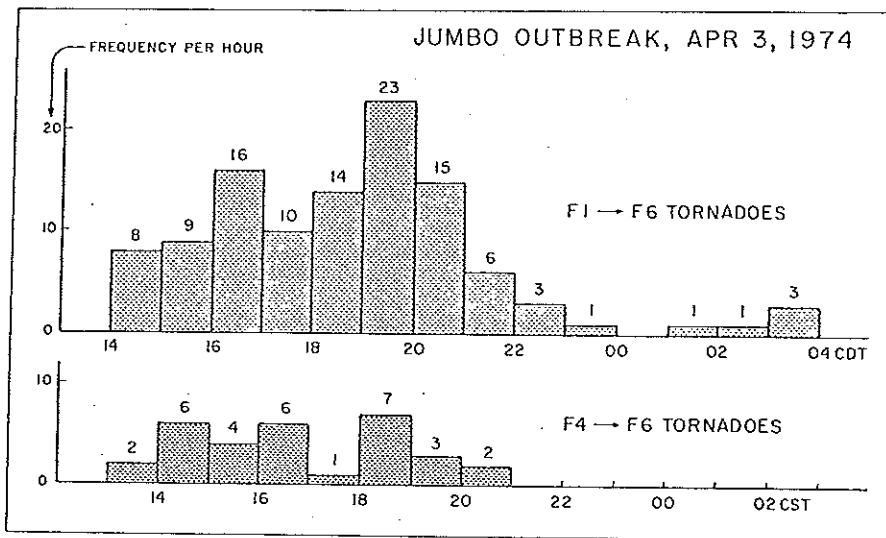


Fig. 5. Diurnal variation of tornado occurrences. April 3-4, 1974.

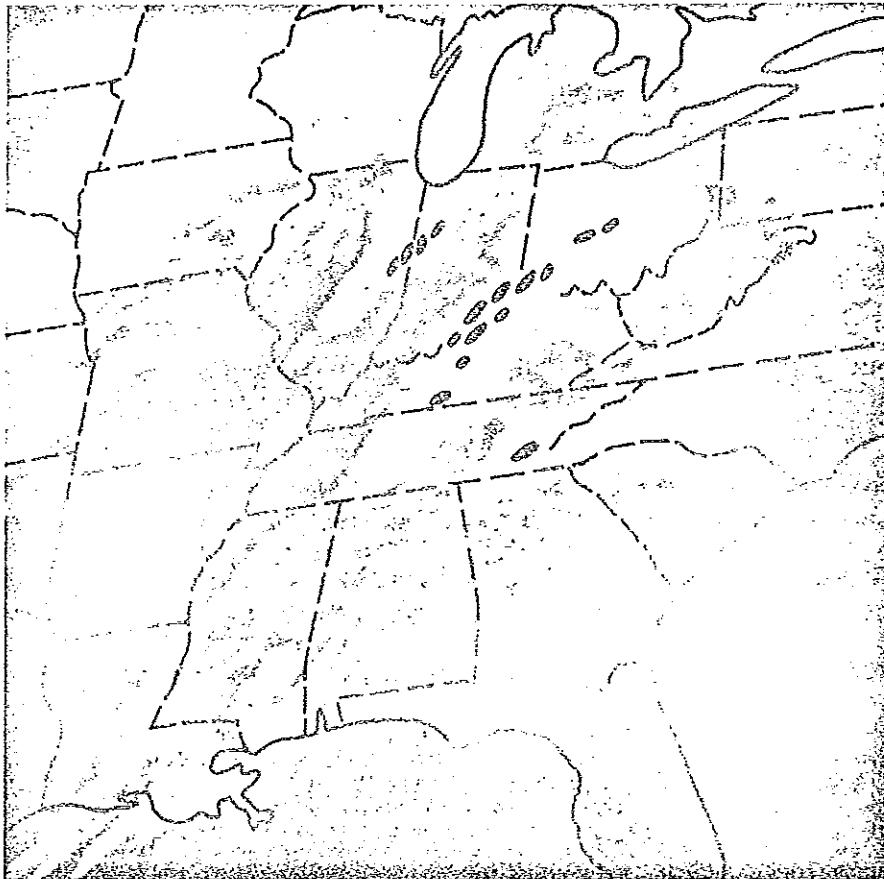


Fig. 6. 16 tornadoes which occurred in one-hour period, 16-17 CDT. Tornado locations are superimposed on the ATS picture taken at 1617 CDT.



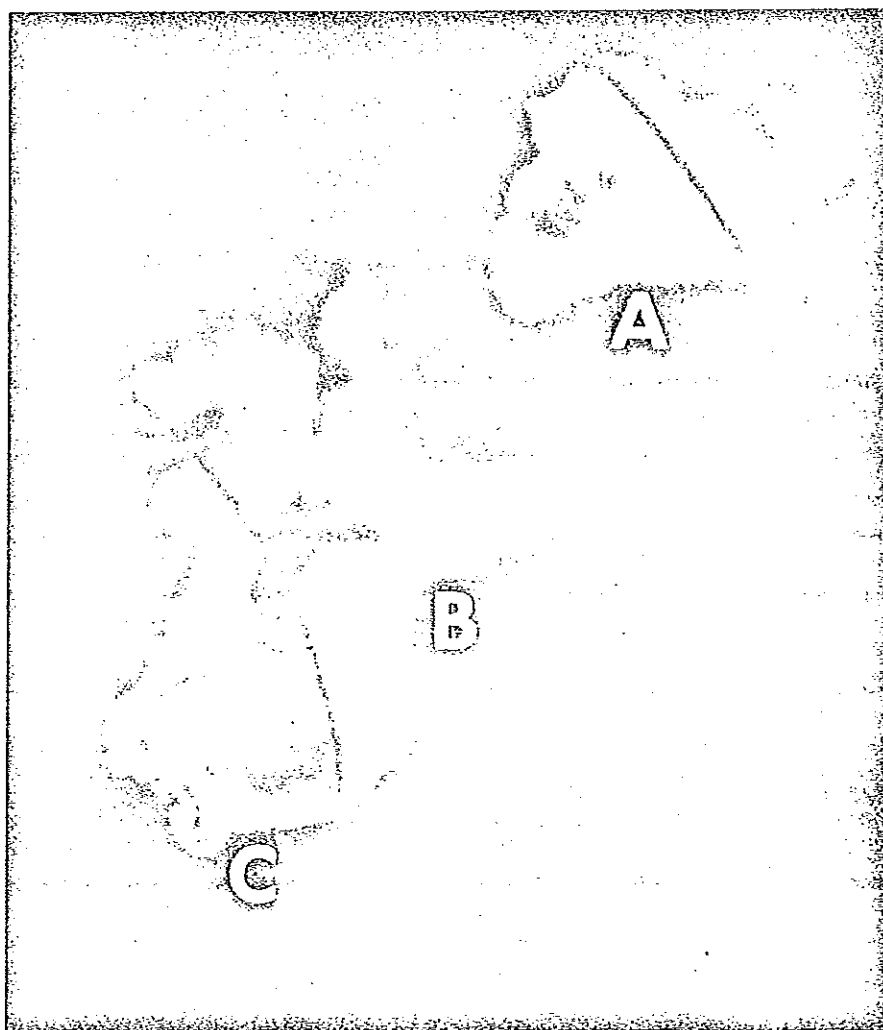


Fig. 7. Three hook-echo cells photographed by Evansville WSR-57 radar.  
Range-mark interval is 25 nautical miles. Picture time 1422 CDT.

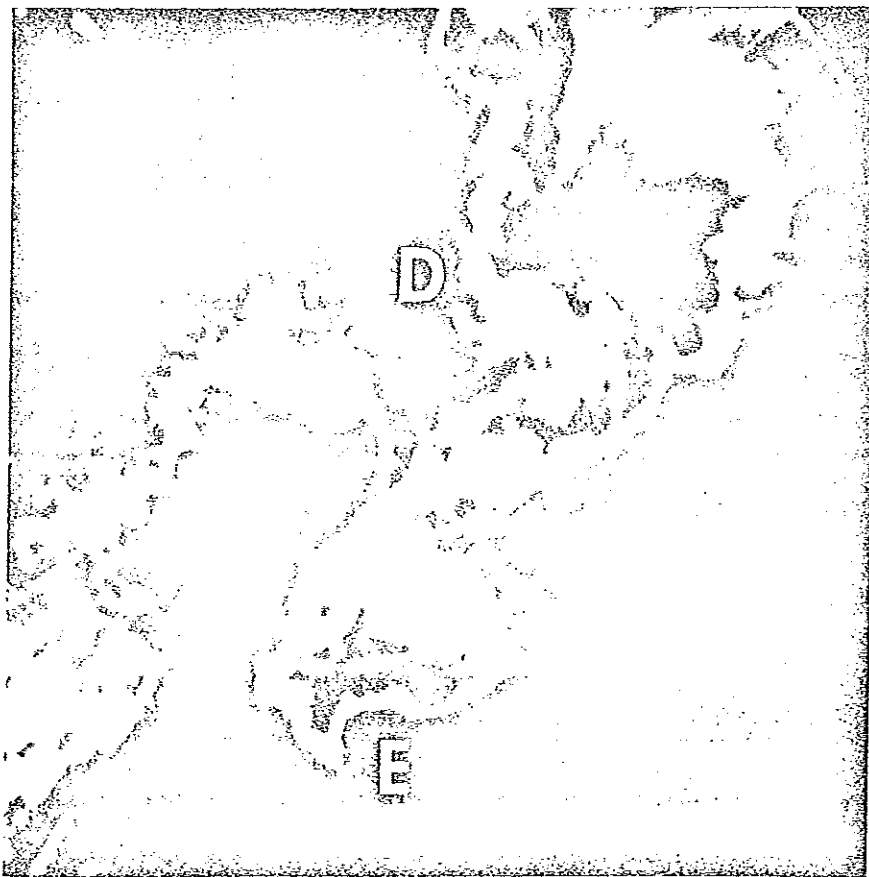


Fig. 8. Hook echoes photographed by Illinois State Water Survey. The Sidney tornado (No. 5) rated as F2 was in progress beneath echo D. Our aerial survey failed to find F1 or worse damage over the area of hook echo E. Range-mark interval, 20 N.M. Picture time 1606 CDT. Courtesy of Changnon and Morgan (1974).

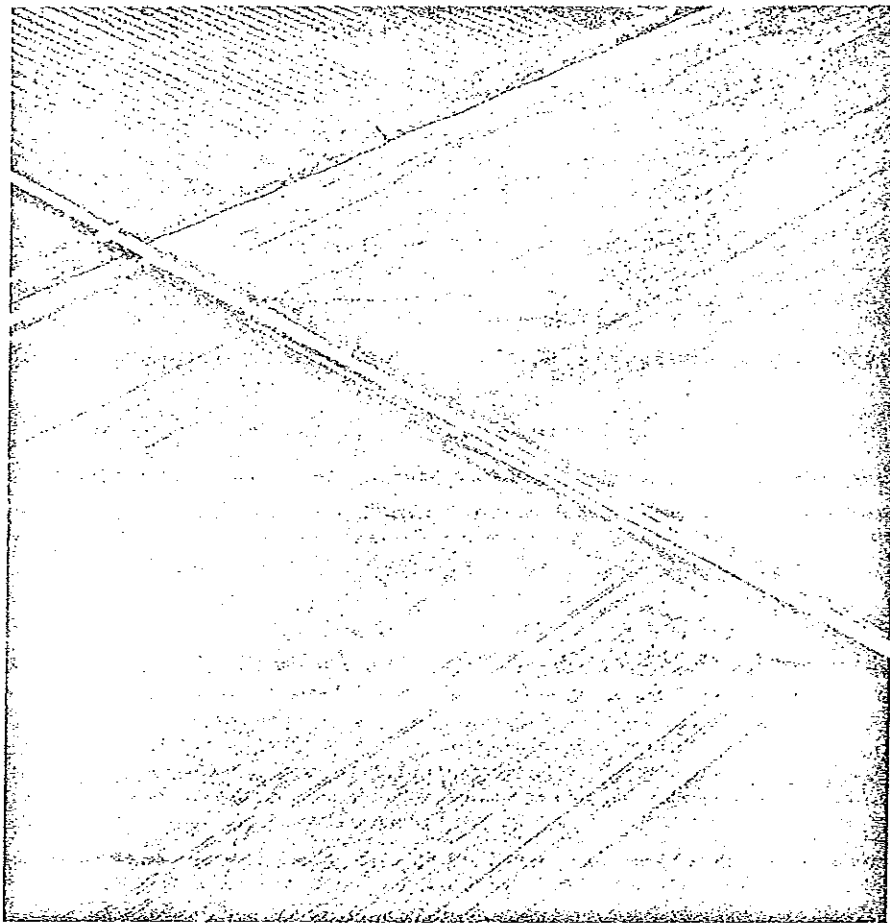


Fig. 9. Cycloidal marks left by the Anchor tornado (No. 2). Maximum translational speed of suction vortices is estimated to be 180 mph.

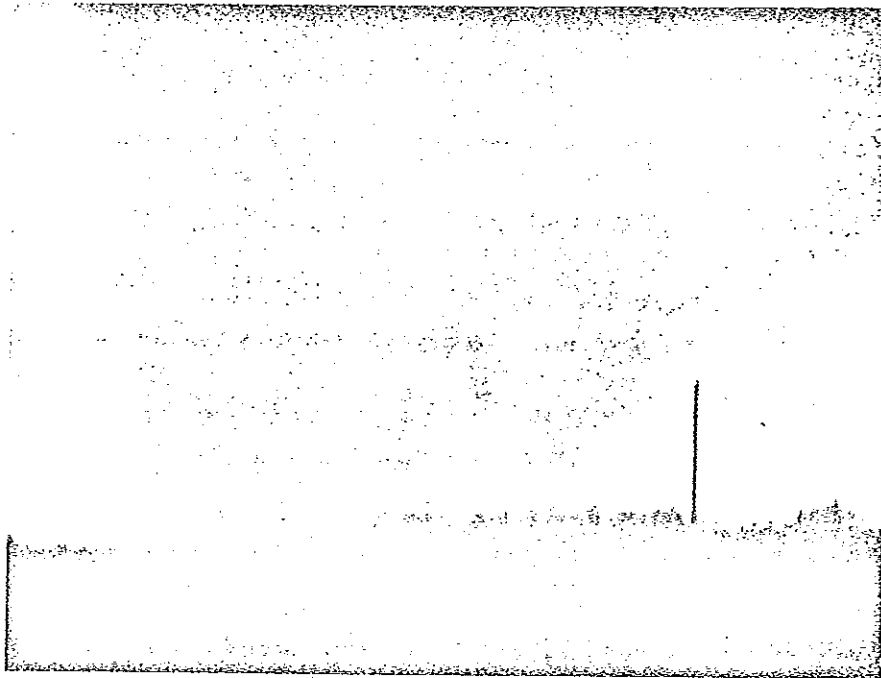


Fig. 10. Three suction vortices rotating around the common center of Muncie tornado (No. 21) at 1546 CDT, April 3, 1974. Courtesy of Mr. Hubbard WISH-TV cameraman-correspondent.

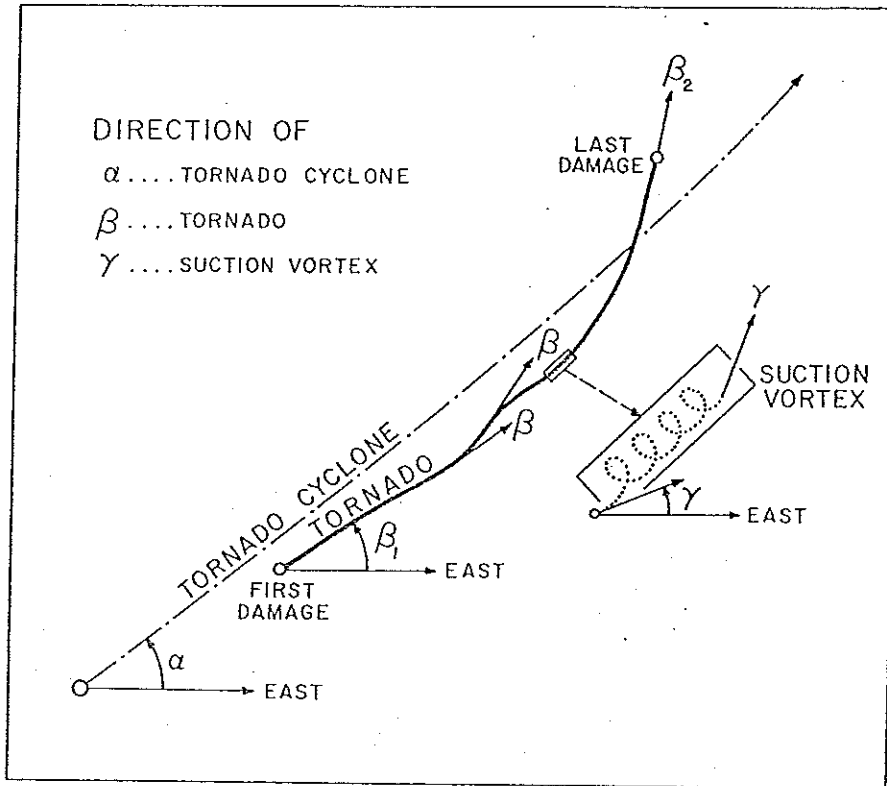


Fig. 11. Definition of the direction of three types of circular vortices, tornado cyclone, tornado, and suction vortex.

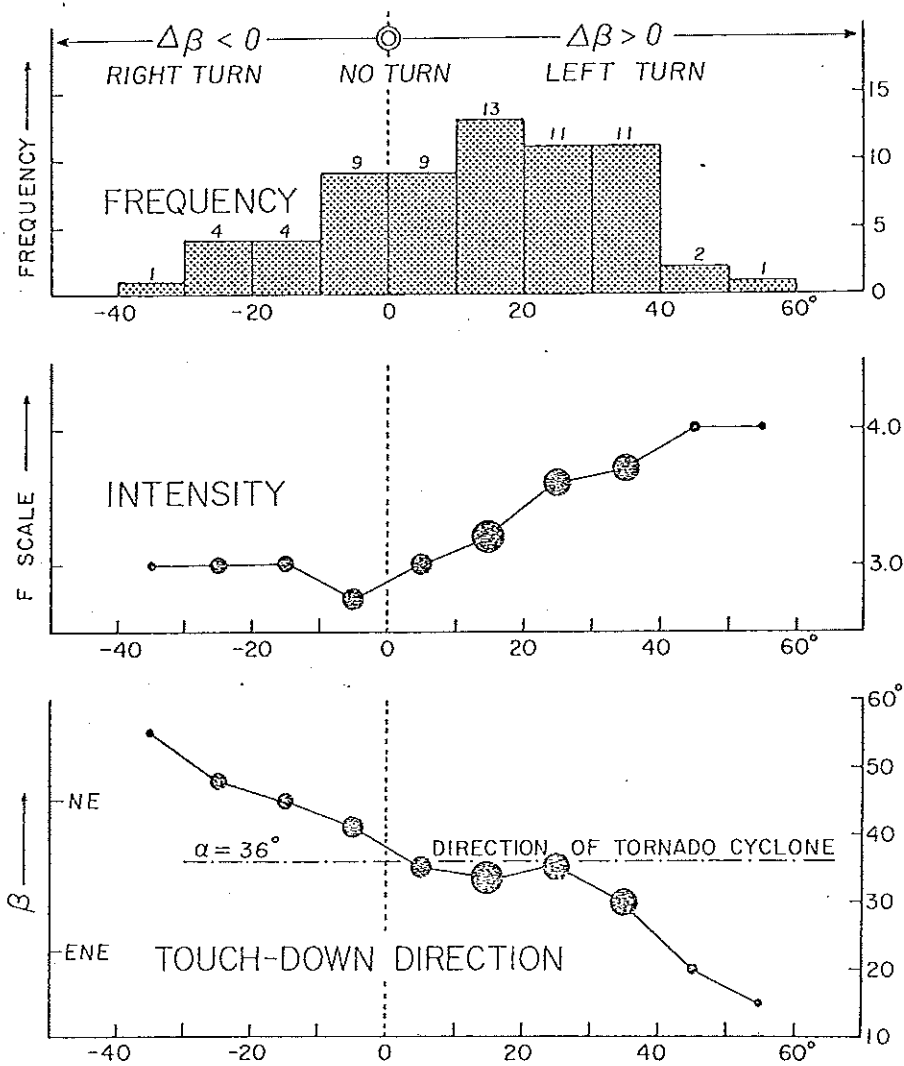


Fig. 12. Turn angles of Jumbo-outbreak tornadoes. On the average left-turn tornadoes were more intense than their right-turn counterparts.

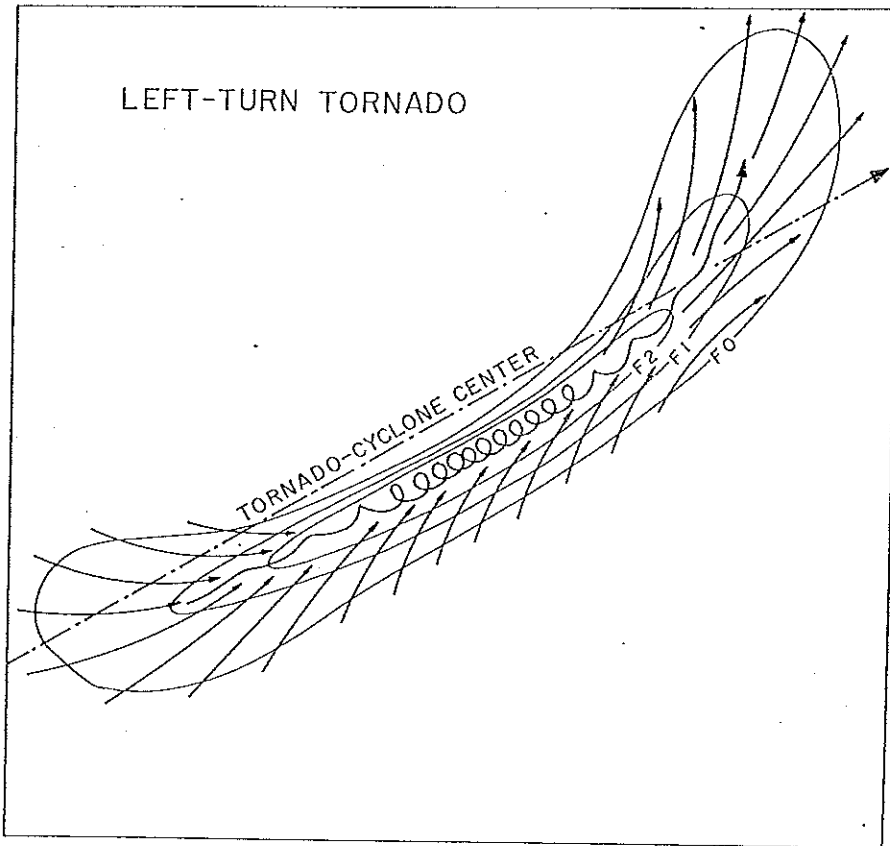


Fig. 13. A model of the left-turn tornadoes.

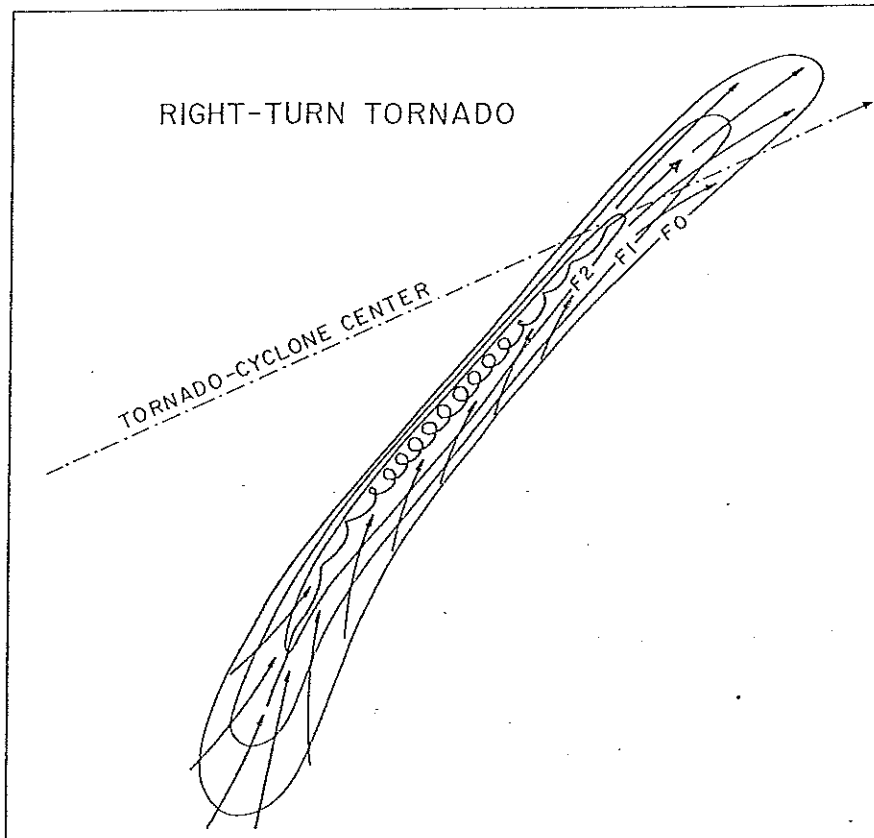


Fig. 14. A model of the right-turn tornadoes.



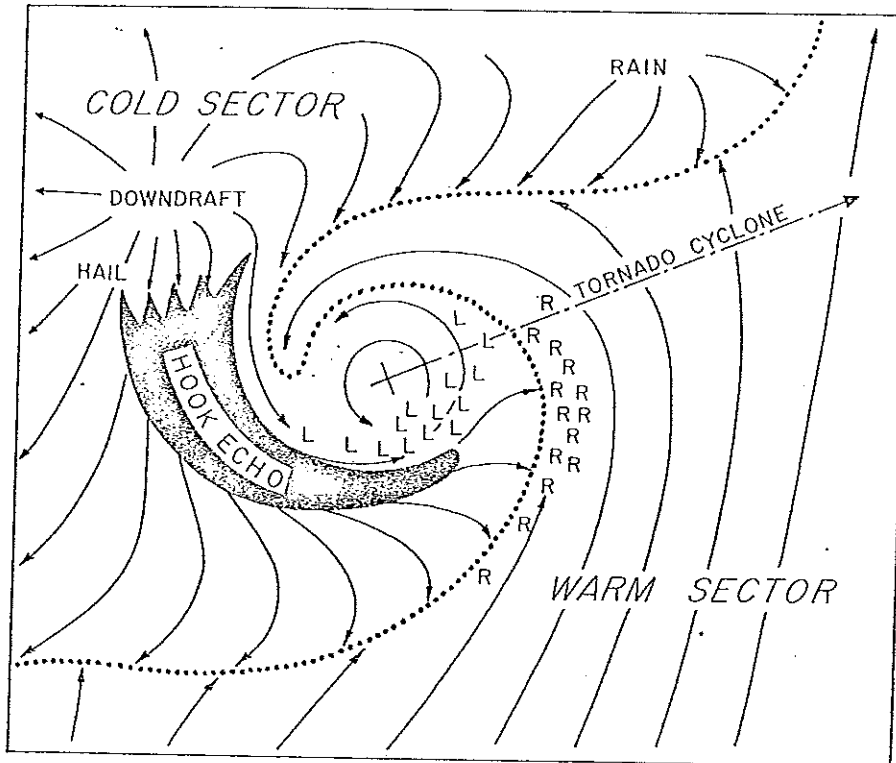


Fig. 15. Schematic view of a tornado cyclone at the surface and the preferable locations of left-turn (L) and right-turn (R) tornadoes.

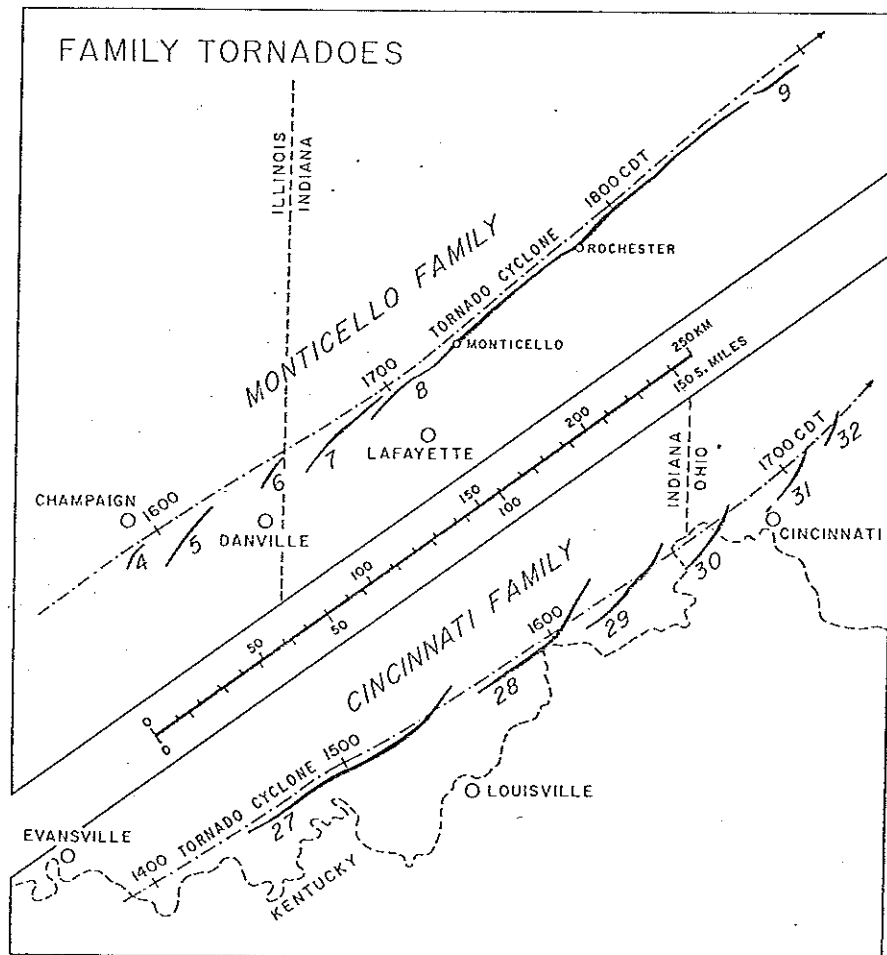


Fig. 16. Monticello tornado family with right-turn tornadoes and Cincinnati family with left-turn tornadoes.

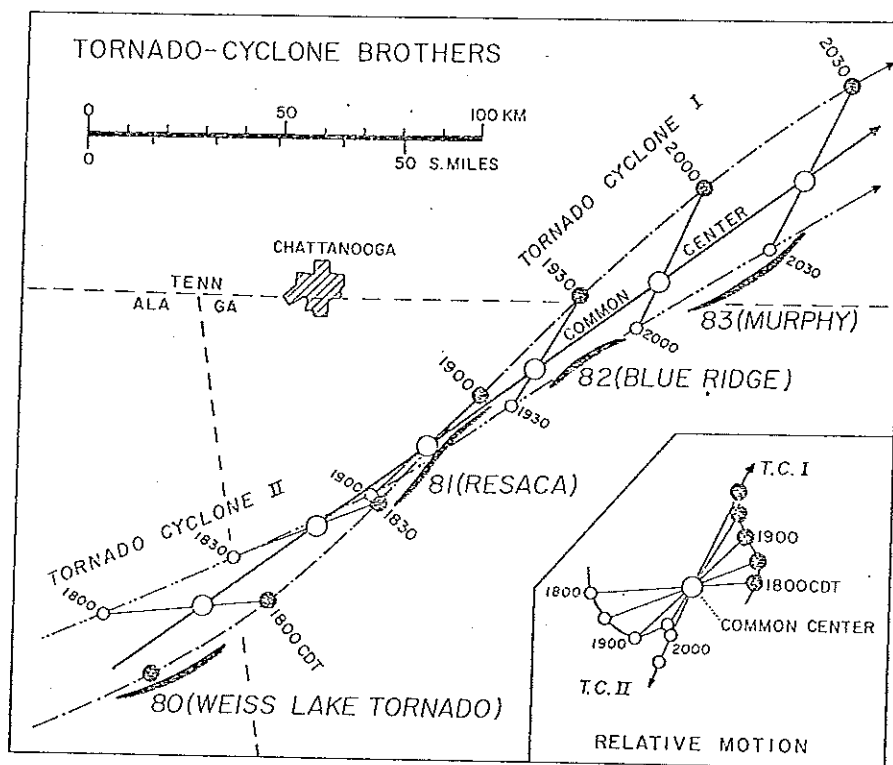


Fig. 17. Four cousin tornadoes spawned from tornado cyclone brothers. Tornadoes 80 and 81 moved over rolling hills while 82 and 83 crossed ridges and tops of mountains. These tornadoes were rated as F4, F4, F3, and F4, respectively.